Extended Noise theory of GaAs-Schottky-Diodes

Frank Gottwald
Institut für Hochfrequenztechnik
Universität Hannover

Abstract- An extended analysis is presented for the excess noise of GaAs-Schottky-Diodes in a mm-waveguide-mixer. A mixer simulation program includes the effects of nonlinear capacitances, arbitrary embedding impedances, non ideality of microwave diodes and all kinds of noise generated in the diode. The determination of the diode capacitance is established in an empirical way. With the measurement of both, the noise at 94 GHz and the conversion loss, it is possible to find a new characteristic of the capacitance versus voltage. This differs from the commonly used square root function. Based on measurements of the noise temperature for different currents in the frequency range of 100 MHz to 94 GHz a noise model of the diode is established and compared to conventional noise theory: In the frequency range below 2 GHz the noise temperature runs through a maximum with respect to diode current; with the frequency increased the maximum decreases and is shifted to higher currents. This effect can be modeled by a current dependent time constant in the trapping noise formula. Finally measurements at an original 94 GHz mixer were done to verify the theoretical results including the extensions mentioned above. Calculated and measured values of conversion loss and noise temperature agree in an excellent manner.

I. Introduction

Two GaAs-Schottky-Diodes were used for the presented experimentally and theoretically analysis. These diodes were fabricated at the TU Darmstadt [1] and indicated as DA357-1 and D644-08 with the anode diameters 1,5µm and 0,8µm respectively. Both consists of a high doped substrate layer (N_{depi}, d_{epi}) and a lower doped thin epitaxial layer (N_{dsub}, d_{sub}), see table 1. Pt/Au is used as the anode material. The determination of the diode parameters are established from the DC-characteristics.

	N_{depi}	N_{dsub}	d_{epi}	d_{sub}	R_S	n	C_{j0}	C_j
DA-357-1	8e16 cm^{-3}	3e18 cm^{-3}	140nm	70 µm	10 Ω	1,44	2,5 fF	14 fF
D644-08	4,5e17 cm^{-3}	3e18 cm^{-3}	53 nm	70 µm	9,8 Ω	1,31	1,5 fF	8,5 fF

Table 1: Series resistance R_S, ideality factor n, zero bias capacitance C_{j0}, biased capacitance C_j

The measurement of the diode noise and the determination of the noise temperature of the diodes is presented. In the frequency range below 20 GHz the noise temperature is calculated

by using the Y-method. A Dicke-Radiometer is used for the measurement of the noise temperature at 94 GHz. The diode chip is placed at the end of a coaxial low pass filter of a mm-waveguide-mixer. The Dicke-Radiometer is connected to the waveguide port and the coaxial port is used for the measurement at frequencies below 20 GHz. The reflection coefficient has to be determined to calculate the noise temperature. Based on measurements of the noise temperature for different currents in the frequency range of 100 MHz to 94 GHz a noise model of the diode is established and compared to conventional noise theory: In the frequency range below 2 GHz the noise temperature runs through a maximum with respect to diode current; with the frequency increased the maximum decreases and is shifted to higher currents. This behavior is not published and so far not mentioned in the literature. The outlined effect can be modeled by a current dependent time constant in the trapping noise formula.

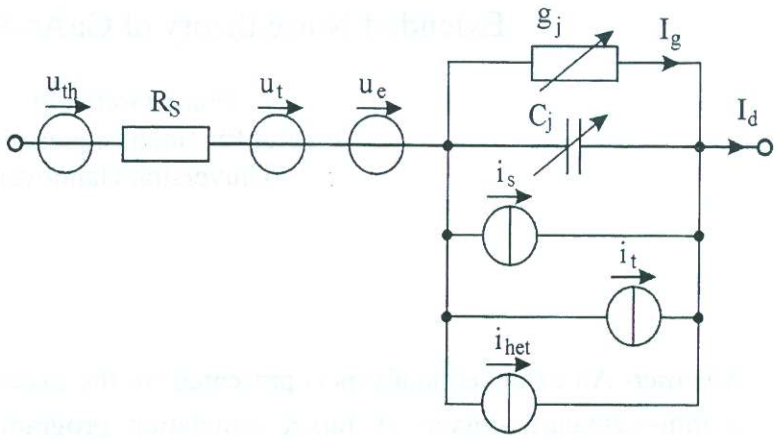

Figure 1: Diode noise model

II. New noise source

This new noise source and the well known noise sources are integrated in an extended noise model of the diode. This model describes the noise temperature in the frequency range of 100 MHz to 94 GHz. The new noise source combines the trapping-noise and the hot-electron-noise and is called hot-electron-trapping. The proposed new noise source is derived of the dependence of velocity, temperature and life time of electrons, and is described in Eq. (1). The physical explanation of the derived noise source is the shorter stay of hot electrons in the traps; the time constant decreases with respect to hotter electrons. The traps become more shallow to electrons with high energy. The trapping time constant therefore becomes temperature- or energy-dependent. The extended noise model is shown in figure 1. The single noise sources are thermal noise u_{th}, shot noise i_S, hot-electron-noise u_e, trapping noise u_t and i_t and the new proposed hot-electron-trapping i_{het}. Here only the derivation of the hot-electron-trapping noise source is shown.

Sze [2] gives an expression of the dependence of the minority carrier life time from the electron velocity. Furthermore the relation contains the thermal velocity which depends on the electron temperature. Despite of the validity for minority carriers the relation was used for the majority carriers which are dominant in GaAs.

The electron energy and temperature T_e increases because of the increasing diode current. The electron temperature is calculated with the relation of energy preservation [3], Eq. (1).

$$\frac{dW}{dt} = qEv_d - (W - W_0)/\tau_e \qquad (1)$$

Here W and W_0 are the electron energies with and without electrical field E. v_d is the drift velocity of the electrons and τ_e is the energy relaxation time. q is the electron charge. The observed bend in the noise temperature occurs at higher diode currents, so the current dependent electron mobility is taken into account.
If we assume the system is in equilibrium, then the differentiation of the energy W disappears. The drift velocity of the electrons is

$$v_d = E\mu(E) = \frac{I}{q \cdot N_{depi} \cdot A}. \tag{2}$$

The electron energy is calculated with the following relation:

$$W = \frac{3}{2} kT_e. \tag{3}$$

After some derivations the electron temperature is calculated,

$$qEv_d = \frac{3k}{2\tau_e}(T_e - T_0) = q\frac{(E\mu(E))^2}{\mu(E)} = \frac{1}{q\mu(E)}\frac{I^2}{A^2 \cdot N_{depi}^2} \tag{4}$$

and then

$$T_e = T_0\left(1 + \frac{2\tau_e}{3qk\mu(E)T_0}\left(\frac{I}{AN_{depi}}\right)^2\right). \tag{5}$$

The field dependent electron mobility $\mu(E)$ is translated in a current dependent mobility $\mu(I)$ because of the relation between electrical field and diode current. This new current dependent electron temperature is inserted in the relation given by Sze, Eq. (6).

$$\tau_{het} = 1/\left(\sigma N_{het}\sqrt{3kT_e/m^*}\right) \tag{6}$$

Here m* is the effective electron mass, N_{het} is the trap density and σ is the capture cross section. This new current dependent time constant then is inserted into the known trapping noise formula [4,5], Eq. (7). The new noise source is attached as a current source parallel to the diode junction, see figure 1.

$$\left\langle i_{het}^{\,2}\right\rangle = 2 \cdot K_{het,n}(f)\Delta f \qquad \text{with} \qquad K_{het,n} = \sum_{n=1}^{N} \frac{N_{het,n}}{N_{depi}} \frac{\tau_{het,n} I^2}{1 + (\omega\tau_{het,n})^2} \tag{7}$$

N is the number of different noise sources with different coefficients. Some quantities are material or production dependent, as trap densities and time constants. These values can only be determined by noise measurements and fitting algorithms. The physical constants are calculated with a mixture of the simulated annealing algorithm and a kind of gradient method. The measured and calculated noise temperatures are shown in the following figures 2 and 3 for the diode DA357-1 with an anode diameter of 1,5µm and D644-08 with an anode diameter

of 0,8µm, respectively. The measured temperatures are presented as crosses. The lines are the results of simulation after a successful fitting of parameters. The differences between measurement and calculation are in the tolerance range obtained from an error calculation taking the reflection and noise measurement into account.

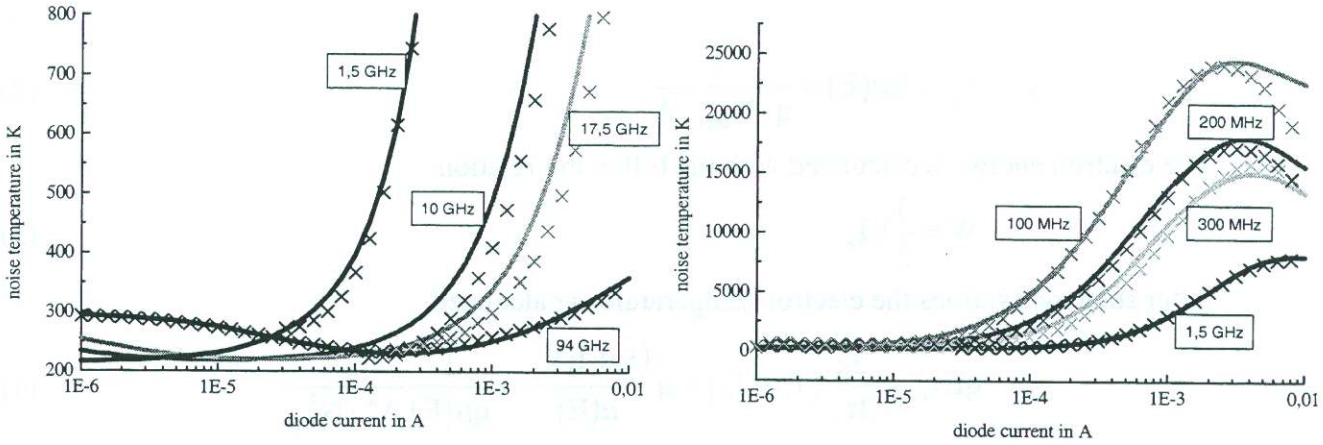

Figure 2: Comparison of the measured (crosses) and calculated (lines) noise temperature of the diode DA357-1.

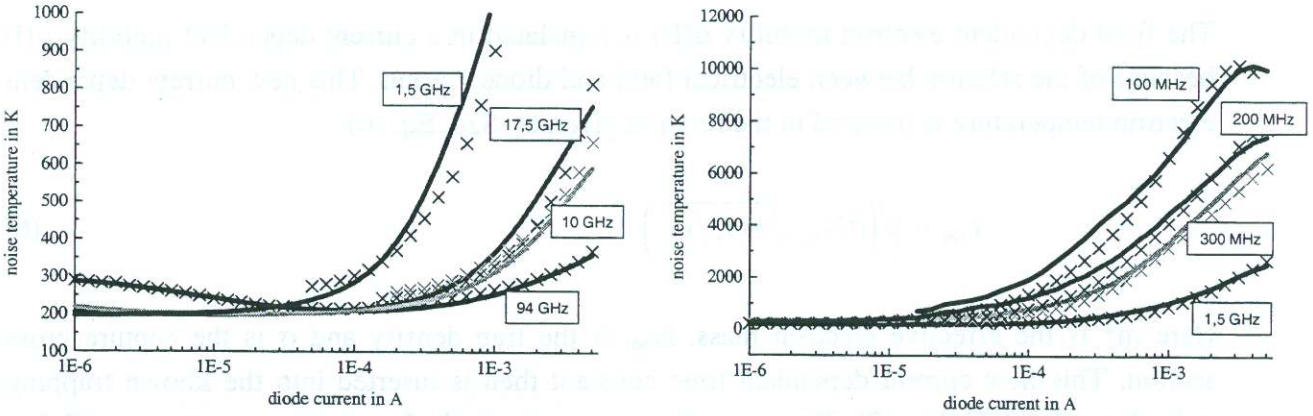

Figure 3: Comparison of the measured (crosses) and calculated (lines) noise temperature of the diode D644-08.

The calculation of the total noise temperature is done in the following matter.

$$P_{verf} = kT_d\Delta f = \left[\left\langle u_{th}^2\right\rangle + \left\langle u_t^2\right\rangle + \left\langle u_e^2\right\rangle + \left(\left\langle i_S^2\right\rangle + \left\langle i_t^2\right\rangle + \left\langle i_{het}^2\right\rangle\right)\cdot\frac{r_j^2}{1+(\omega r_j C_j)^2}\right] \Big/ \left(4\cdot \mathrm{Re}\{\underline{Z}_{ges}\}\right)$$

$$\text{with}\quad \mathrm{Re}\{\underline{Z}_{ges}\} = R_s + \frac{r_j}{1+(\omega r_j C_j)^2}. \qquad (8)$$

III. Determination of diode capacitance

In the description of equation (8) the value of the diode capacitance in the forward bias region is needed. To fit the calculated noise temperature curve at 94 GHz, the capacitance is also obtained by variation of parameters using the mentioned optimization method. The capacitance of a forward biased diode C_j in the voltage range of 0,25 to 0,5 V is approximately four to five times higher than the calculated capacitance at zero bias C_{j0}.
Furthermore the noise temperature and the conversion loss of a harmonically pumped mm-waveguide-mixer are investigated. Additional a mixer simulation program was built including the correlation of all different noise sources. The waveguide mixer has a sliding backshort to match the diode impedances. The conversion loss of the mixer was measured at different backshort positions. The mixer simulation program uses the harmonic balance method to establish the conversion matrix. This method needs the capacitance of the forward biased diode. The curve of the interesting capacitance range is empirically determined by consideration of the calculated capacitance at zero bias and the fitted capacitance at forward bias mentioned above. Some possible capacitance curves and the commonly used square root function are shown in figure 4. These curves are inserted in the mixer simulation program and the results are compared with the measured conversion losses at different backshort positions. Figure 4 also shows the curves of the conversion loss simulated for different capacitance curves C_0 to C_3 respectively. The best agreement to the measurement shows the curve C_0 [6]. The square root function C_3 does not deliver good results. The capacitance curve of a forward biased diode possesses finite values near the barrier potential in the way shown in figure 4 and differs from the square root function. Voltages U_j higher than approximately the barrier potential do not occur, because the current dependent diode conductance g_j short circuits the capacitance.

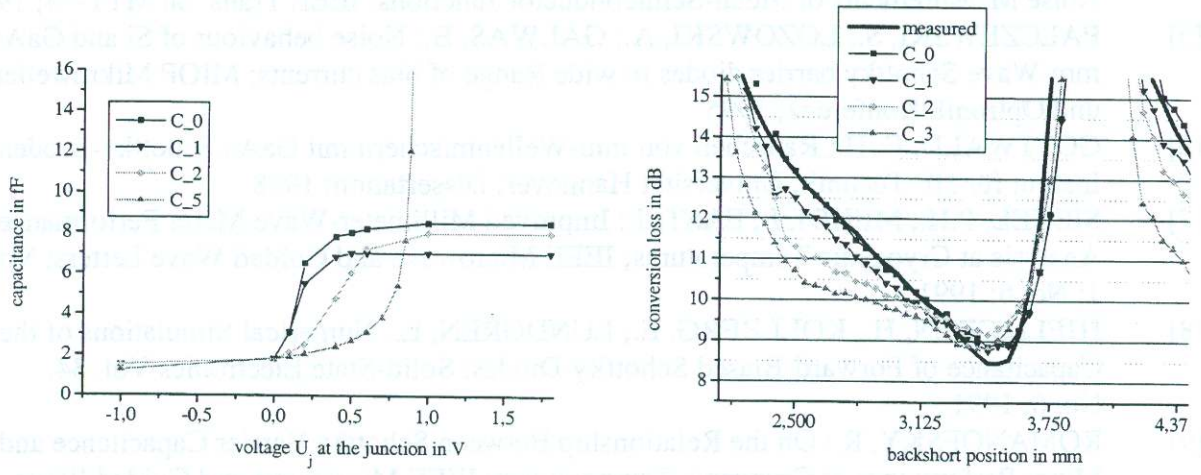

Figure 4: Some in the mixer simulation program inserted capacitance curves and the calculated conversion losses respectively. Results for the diode D644-08.

This capacitance curve is also used for the simulation of the diode noise at 94 GHz. Figure 5 shows the comparison of measured and calculated values. The calculation is done with Eq. (8), however only frequency and current independent sources (thermal and shot noise) are considered. The comparison shows are very good match in the decreasing range of the noise

curve. In this range at low currents the excess noise does not occur. At high currents the two values diverge because of the previously explained conditions.
These results are comparable with the results of Siegel [7], Hjelmgren [8] and Romanofsky [9].

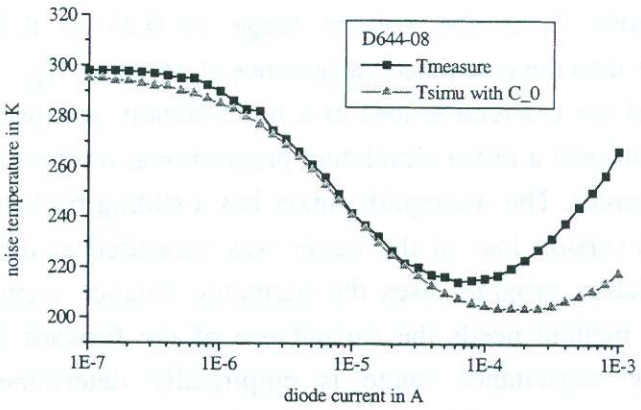

Figure 5: Comparison of the measured and simulated noise at 94 GHz. Equation (8) uses the capacitance curve C_0, shown in figure 4.

IV. Literature

[1] GRÜB, A.: Technologieentwicklung für Terahertz-Schottkydioden und Nanometerstrukturen; VDI-Verlag; 1992

[2] SZE, S.M.: Physics of Semiconductor Devices; John Wiley & Sons; 1981

[3] ZIRATH, H.: High-frequency noise and current-voltage characteristics of mm-wave platinum n-n+-GaAs Schottky barrier diodes; J. Appl. Phys. 60 (4); 1986

[4] JELENSKI, A.; KOLLBERG, E.; ZIRATH, H.: Broad-Band Noise Mechanisms and Noise Measurements of Metal-Semiconductor Junctions; IEEE Trans. on MTT-34; 1986

[5] PALCZEWSKI, S.; LOZOWSKI, A.; GALWAS, B.: Noise behaviour of Si and GaAs mm-Wave Schottky barrier diodes in wide Range of bias currents; MIOP Mikrowellen und Optronik Konferenz; 1995

[6] GOTTWALD, F.-H.: Rauschen von mm-Wellenmischern mit GaAs-Schottky-Dioden; Institut für HF-Technik; Universität Hannover; Dissertation; 1998

[7] SIEGEL, P.H.; MEHDI, I.; EAST, J.: Improved Millimeter-Wave Mixer Performance Analysis at Cryogenic Temperatures; IEEE Microwave and Guided Wave Letters; Vol. 1; No. 6; 1991

[8] HJELMGREN, H.; KOLLBERG, E.; LUNDGREN, L.: Numerical Simulations of the Capacitance of Forward-Biased Schottky-Diodes; Solid-State Electronics Vol. 34; No. 6; 1991

[9] ROMANOFSKY, R.: On the Relationship Between Schottky Barrier Capacitance and Mixer Performance at Cryogenic Temperatures; IEEE Microwave and Guided Wave Letters; Vol. 6; No. 8; 1996